Jurnal Geosaintek Vol 11. No. 1. Tahun 2025. 1-99. p-ISSN : 2460-9072, e-ISSN : 2502-3659

REAL-TIME CORRELATION ANALYSIS MONITORING SLOPE MOVEMENT USING SLOPE STABILITY RADAR (SSR605-XT) WITH ROCK MASS RATING AND ALTERATION TYPE DATA

R. Andy Erwin Wijaya[1], Bayurohman Pangacella Putra[1], Tesya Puspita Mamonto[1]
[1]Program Studi Teknik Pertambangan, Fakultas Teknik dan Perencanaan , Institut Teknologi Nasional Yogyakarta
e-mail: andyerwin@itny.ac.id

Abstrak. Lokasi Pit North Main Ridge adalah area penambangan emas terbuka dengan beberapa jenjang dan lereng yang curam, yang memiliki potensi menyebabkan longsor. Oleh karena itu, pemantauan pergerakan lereng sangat penting untuk mengurangi risiko longsor dan memastikan kegiatan penambangan berjalan dengan aman. Pemantauan ini menggunakan metode real-time secara langsung di dalam lubang tambang dengan menggunakan alat Slope Stability Radar (SSR605-XT). Data yang diperoleh dari pemantauan radar sekitar 2 bulan dianalisis menggunakan perangkat lunak IQ Monitor untuk mendapatkan informasi mengenai deformasi dan kecepatan pergerakan lereng. Pemetaan di dalam lubang tambang dilakukan dengan mengukur jarak 5 meter untuk setiap segmen, dengan total panjang 575 meter yang dibagi menjadi 115 segmen. Kondisi lokasi pemantauan di lereng tambang, yang ditandai dengan pergerakan lereng yang signifikan, sangat dipengaruhi oleh data estimasi penilaian massa batuan dan jenis alterasi. Semakin lemah kelas massa batuan (3 dan 4) dan mempunyai tipe alterasi argillic, maka berpotensi terjadinya pergerakan lereng. Sebaliknya semakin kuat kelas massa batuan (1 dan 2) dan mempunyai alterasi silicic dan advanced argillic, maka pergerakan lereng semakin berkurang.
Kata Kunci: alteration; monitoring; Rock Mass Rating; slope stability radar

Abstract. *The North Main Ridge Pit location is an open gold mining area with several benches and steep slopes, which have the potential to cause landslides. Therefore, monitoring slope movements is crucial to reducing landslide risks and ensuring safe mining activities. This monitoring utilizes real-time methods directly within the mine pit using the Slope Stability Radar (SSR605-XT) tool. Data obtained from radar monitoring is analyzed using the IQ Monitor software to acquire information on slope deformation and movement speed. Mapping within the mine pit is conducted by measuring a distance of 5 meters for each segment, with a total length of 575 meters divided into 115 segments. The condition of the monitoring site at the mining level, characterized by significant slope movements, is heavily influenced by data estimates of rock mass assessment and alteration types. The weaker the rock mass class (3 and 4) and the argillic alteration type, the potential for slope movement to occur. On the other hand, the stronger the rock mass class (1 and 2) and the silicic and advanced argillic alteration, the less slope movement.*
Keywords: *monitoring; Rock Mass Rating; slope stability radar; alteration*

INTRODUCTION

In recent years, numerous researchers have delved extensively into the intricacies of rock mechanisms (Chen et al., 2023). The analysis of slope stability has consistently remained a complex and pivotal concern within the realm of earth geotechnical engineering (Huang et al., 2024). PT. J Resources Bolaang Mongondow is a company engaged in gold mining operations, employing the open-pit method, which involves excavating minerals along a relatively horizontal surface descending towards the mineral deposits, employing a tiered mining approach. Slope stability stands as a critical subject in engineering geology, boasting a rich history spanning centuries. In geotechnical engineering, accurately gauging the safety factor of a slope to avert failure is of paramount importance (Kumar et al., 2023). Slope stability analysis is a critical step in many mining and geotechnical engineering projects, including open-pit mining, embankments, earth dams, landfills, and highways (Zheng et al., 2024). Undertaking such analysis prior to slope alteration is indispensable for devising and executing mitigation strategies aimed at preventing further slope deterioration (Al-E'Bayat et al., 2024).

DOI : http://dx.doi.org/10.12962/j25023659.v11i1.1882
Artikel Masuk : 25-07-2024 Artikel Diulas : 13-11-2024 Artikel Diterima : 09-04-2025

Characterizing rock mass and analyzing rocky slope stability are essential for ensuring user safety (Delgado et al., 2023). Analyzing slope stability in rock masses is complex due to inherent uncertainties and risks (Jia et al., 2023). Assessing landslide susceptibility and hazards in mountainous regions is crucial for managing regional landslide risk. Slopes subjected to gravity can collapse when faced with unfavorable morphology, lithology, structure, or various triggering factors (Kundu et al., 2023).

Slope stability is one of the important topics in engineering geology that has been studied for more than 300 years. Various stability assessment methods have been developed, including limit equilibrium analysis, numerical methods, as well as probabilistic and statistical approaches to determine the factor of safety (F.S) and potential failure mechanisms (Azarafza et al., 2021). Slope stability is a vital concern for safety and production in open-pit mines. Slope stability monitoring techniques track minor initial movements before a landslide occurs. These systems can detect wall deformation with sub-millimeter accuracy and high spatial resolution (Reeves et al., 2001). Adhitama et al. (2021) provide suggestions for geotechnical monitoring and analysis activities by carrying out routine measurements with convergence tools in the research area and monitoring. This slope-monitoring system can use robotic devices and geotechnical sensors (Vasilev & Toshkov, 2016), and slope stability monitoring also considers geological and topographic conditions (Boyle et al., 2014; Yang et al., 2024). Making mining slopes on rocks that are manageable can cause landslide problems. This can result in accidents for mining workers and damage to heavy equipment at the mining front. Companies must improve security to reduce landslide potential (Sulistio & Wijaya, 2022). Slope stability is considered a significant problem. Also, slope failure can cause psychological damage, including loss of property and human lives worldwide (Moayedi et al., 2021; Kumar et al., 2023).

The safety of mining operations depends on effective mine design. This design is influenced by the quality of the rock mass, which varies between different mining sites based on geological conditions (Wijaya et al., 2014). To categorize rocks, the rock mass classification system is used, which has been applied in various engineering projects and stability studies. This system focuses on rock mass parameters and their applications in engineering, such as tunnels, slopes, and foundations. Rock mass classification is particularly beneficial in locations where sample collection and observation are challenging (Qazi & Singh, 2023).

Natural rock masses form in specific geological contexts and are made up of many rocks and structural planes with variable properties. When these rock masses are integrated into the foundations of dams, slopes, and underground structures, they become engineered rock masses with both natural and engineered features. Due to their complexity, engineered rock masses are classified into different categories based on rock mass quality and stability, guided by rock engineering characteristics and practical experience (Wu et al., 2023a).

The Modified Slope Mass Rating (M-SMR) system has been successfully utilized in re-proposing slope levels (Abd Rahim et al., 2023). The occurrence of unforeseen slope failures in surface mines prompted the creation of various monitoring instruments for pit slopes. Among these tools utilized for continuous monitoring of open-pit mine slopes is the slope stability radar (SSR) (Gong et al., 2021). SSR is a technology that can monitor strata movements effectively (Kumar, 2020; Wang et al., 2024). SSR is a technology capable of effectively monitoring movements within rock strata (Kumar, 2020; Wang et al., 2024). The Slope Stability Radar (SSR) system provides continuous surveillance of pit walls and has the capability to identify slope deformations at a sub-millimeter scale (Shellam & Coggan, 2020). Utilizing electromagnetic waves, slope stability radar (SSR) serves as a technological tool for monitoring slope stability. Swift and accurate predictions of slope stability are vital for ensuring safe operations and cost-efficient maintenance of slopes (Zheng et al., 2024). Slope Stability Radar is adept at detecting and interpreting movements within steep and unstable pits (Saunders et al., 2016). Monitoring findings are presented in the form of trends or graphs and are subsequently analyzed. Key elements for geotechnical monitoring include slope control points determined through GPS or total

DOI : http://dx.doi.org/10.12962/j25023659.v11i1.1882

Artikel Masuk : 25-07-2024 Artikel Diulas : 13-11-2024 Artikel Diterima : 09-04-2025

station, visual inspections, and geotechnical instruments. These factors play a crucial role in guiding subsequent actions based on standard operating procedures to mitigate potential landslides. This type of alteration influences slope stability through changes in the mechanical properties of rocks, the formation of weak zones, and increased water interaction with the rock mass. Rock alteration in a geotechnical context is significant for designing stable slopes, especially in open-pit mining areas (Kumar & Rathee, 2017).

Slope stability radar is used in open-pit mines to monitor slope movements effectively. This technology employs sensors and computerized analysis techniques in a variety of geotechnical sectors to reduce negative impacts and prevent early mine design failures, guaranteeing that mining activities may continue safely (Elmouttie & Dean, 2020). A theoretical framework is crucial for efficiently and cost-effectively monitoring slope stability. According to simulation data, the horizontal movement of slopes peaks around 12 meters from the slope's toe.

RESEARCH METHOD

This research method uses quantitative methods. This research carried out direct observations and measurements in the field. Observations include North Main Ridge pit slope conditions, alteration type, rock mass classification, potential areas prone to landslides at the mine level, and direct slope monitoring. This study examines rock mass classification based on Wijaya and Isnawan's (2015) approach, which assesses landslide potential on mining slope walls by evaluating rock mass strength. The quality of rock masses in open-pit mines can progressively degrade over time due to vibrations from repeated blasting and other mining activities (Saunders et al., 2020). The necessary slope condition data includes slope orientation, rock strength, geological structures, groundwater conditions, and the type of rock forming the slope. Khajehzadeh et al. (2022), who applied ANN and adaptive algorithms, provide a strong foundation for developing a more accurate predictive model to identify landslide potential using real-time data from SSR605-XT. The SSR605-XT radar monitoring captures key data on slope movement, including coordinates, deformation trends, and velocity, offering valuable insights for slope stability assessment. Sampling, observing, and determining the type of rock alteration is vital in geological exploration and mineralization evaluation. Rock samples were taken using drill core samples in several representative locations. Then, the location points are recorded using GPS, followed by a visual description of the rocks and geological structures. Observations were carried out using a megascopic method to determine the physical and mineralogical characteristics of rocks. Then, microscopic analysis, XRD, and chemical analysis will be performed to determine the elemental content and type of mineral. Determining the type of rock alteration is observing the color and process of change due to interaction with hydrothermal fluids and petrographic analysis for alteration minerals.

Data processing is carried out after all the data is complete. Radar monitoring analysis is carried out using Monitor IQ software, which is the basis for creating maps of monitoring location results that display areas that are safe and prone to landslides (Indriastuty et al., 2021).

RESULTS AND DISCUSSION

Research sites

The study is conducted at the PT's North Main Ridge gold mining pit site, which is situated within J Resources Bolaang Mongondow in Bakan Village, Lolayan District, Bolaang Mongondow Regency, North Sulawesi Province.

Characteristics of Rock Masses and Alteration Zones

Over the years, several surveys have been conducted to evaluate the geomechanical characteristics of rock masses within the mining area. Two notable assessments stand out: the first, dating back to 2011, was conducted as part of the mine expansion plan, covering the entire extension and containing extensive data spread across a wide area. The second survey, initiated since 2020, followed the most

DOI : http://dx.doi.org/10.12962/j25023659.v11i1.1882

Artikel Masuk : 25-07-2024 Artikel Diulas : 13-11-2024 Artikel Diterima : 09-04-2025

severe instability events, focusing on enhanced accuracy and attention to identifying zones of weakness (Martinelli et al., 2023). Geotechnical mapping and laboratory testing of rock physical and mechanical properties were employed to characterize the rock masses (Wu et al., 2023b).

The classification of rock masses on mining slopes utilizes the Rock Mass Rating System (RMR) (Bieniawski, 1989; Ganesan & Mishra, 2024). RMR is employed to evaluate rock mass quality, pre-design excavations, and conduct procedures within this framework (Jaiswal et al., 2024). It offers recommendations for underground tunnel support primarily based on empirical dimensional measurements, including those by Terzaghi, Bienawski, and Nick Barton (Wardana & Wijaya, 2021). RMR provides data on numerous rock mass parameters, which are empirically estimated to yield an elemental rock mass RMR value for the first assessment of rock mass quality. Fundamental RMR information is useful in the early stages of slope stability assessment (Singh & Kumar, 2020). RMR is widely used in a variety of engineering disciplines dealing with rocks, including mining, civil tunnel building, hilly terrain highways, bridges, dams, and hydroelectric power projects (Jaiswal et al., 2024).

The research location was observed at several points, each with several segments. Each segment was observed for the characteristics of the RMR rock mass and the type of alteration. The results of the RMR analysis are: Class 2 (29.57%), Class 3 (20%) and Class 4 (50.43%). At the observation location, there are three types of alteration, namely: silicic type (7.94%), advanced argillic (21.43%), and argillic (70.63%). The results of the Rock Mass Rating System (RMR) estimation and alteration type for each observation segment at the North Main Ridge site are shown in (Table 1).

Slope Stability Radar Monitoring Results

Slope stability is a key attribute in geotechnical engineering systems that can be analyzed through the calculation of the factor of safety (Singh et al., 2023). Rock slope stability poses a significant challenge in the field of rock engineering. The mechanical properties of rock masses and discontinuities are difficult to ascertain directly due to scale effects, leading to uncertainties. Additionally, the presence of various failure mechanisms, particularly those involving complex failures, further complicates the process of obtaining viable solutions (Oliveira & Lana, 2023). By utilizing SSR605-XT radar technology, which can detect slope deformation with sub-millimeter accuracy and high spatial resolution, this study integrates real-time data on deformation and slope movement speed with rock mass classification and alteration types. This approach enables the identification of areas with high instability potential, such as expanding plastic zones and significant horizontal displacement, thereby improving the accuracy of landslide prediction and prevention (Liu et al., 2021). In this study, the data collected by the SSR605-XT includes time, maximum deformation, and maximum speed over a specified period. Each pixel selected for analysis represents a division of segments on benches 760, 745, 730, 715, and 705. By monitoring using radar, slope movement stages can be observed to see whether they fall into linear, regressive, and progressive stages. To find out the detailed hourly speed and daily speed, use the VCP60 and VCP1440 settings. Knowing the maximum speed with the VCP60 and VCP1440 settings correlates with the threshold data to determine the risk value. **CP60 and VCP1440** represent different configurations that dictate the operational speeds of a system or process. The maximum speeds allowed by these settings can significantly influence performance and safety metrics. Risk values can be calculated by analyzing historical data related to speed settings and their outcomes. For instance, if data shows that operating at or above the maximum speed of VCP1440 correlates with a high incidence of failures, this can be quantified into a risk value that reflects the potential for loss. **Thresholds** are predefined limits that indicate acceptable levels of performance or risk. They help in identifying when a system operates within safe parameters versus when it may be at risk of failure or inefficiency. When the maximum speed exceeds established thresholds, it raises the likelihood of adverse events. This correlation allows for the assessment of risk values based on how often and by how much these speeds are exceeded. The results of monitoring deformation and speed of slope movement are presented in (Table 2).

DOI : http://dx.doi.org/10.12962/j25023659.v11i1.1882

Artikel Masuk : 25-07-2024 Artikel Diulas : 13-11-2024 Artikel Diterima : 09-04-2025

Table 1. Estimated RMR and Alteration Type at the North Main Ridge Site

No	Location	Segment	RMR Basic	RMR Class	Alteration Type
1	760	A’ – B’	54	3	*Argilic*
2		B’ – C’	54	3	*Argilic*
3		C’ – D’	54	3	*Argilic*
4		D’ – E’	63	2	*Adv. Argilic*
5		E’ – F’	63	2	*Adv. Argilic*
6		F’ – G’	65	2	*Adv. Argilic*
7		G’ – H’	54	3	*Argilic*
8		H’ – I’	54	3	*Argilic*
9		I’ – J’	53	3	*Argilic*
10	745	A’ – B’	32	4	*Argilic*
11		B’ – C’	54	3	*Argilic*
12		C’ – D’	50	3	*Argilic*
13		D’ – E’	38	4	*Argilic*
14		E’ – F’	38	4	*Argilic*
15		F’ – G’	38	4	*Argilic*
16		G’ – H’	38	4	*Argilic*
17		H’ – I’	38	4	*Argilic*
18		I’ – J’	38	4	*Argilic*
19		J’ – K’	38	4	*Argilic*
20		K’ – L’	38	4	*Argilic*
21		L’ – M’	38	4	*Argilic*
22		M’ – N’	38	4	*Argilic*
23		N’ – O’	38	4	*Argilic*
24		O’ – P’	38	4	*Argilic*
25		P’ – Q’	38	4	*Argilic*
26		Q’ – R’	38	4	*Argilic*
27		R’ – S’	38	4	*Argilic*
28		S’ – T’	38	4	*Argilic*
29		T’ – U’	38	4	*Argilic*
30		U’ – V’	38	4	*Argilic*
31		V’ – W’	38	4	*Argilic*
32		W’ – X’	38	4	*Argilic*
33		X’ – Y’	38	4	*Argilic*
34		Y’ – Z’	38	4	*Argilic*
35		Z’ – AA’	38	4	*Argilic*
36		AA’ – BB’	38	4	*Argilic*
37		BB’ – CC’	38	4	*Argilic*
38		CC’ – DD’	38	4	*Argilic*
39		DD’ – EE’	38	4	*Argilic*
40	730	A’ – B’	80	2	*Silicic*
41		B’ – C’	74	2	*Silicic*
42		C’ – D’	74	2	*Silicic*
43		D’ – E’	67	2	*Adv. Argilic*
44		E’ – F’	64	2	*Adv. Argilic*
45		F’ – G’	69	2	*Adv. Argilic*
46		G’ – H’	69	2	*Adv. Argilic*
47		H’ – I’	70	2	*Adv. Argilic*
48		I’ – J’	67	2	*Adv. Argilic*

DOI : http://dx.doi.org/10.12962/j25023659.v11i1.1882

Artikel Masuk : 25-07-2024 Artikel Diulas : 13-11-2024 Artikel Diterima : 09-04-2025

49		J' – K'	69	2	*Adv. Argilic*
50		K' – L'	54	3	*Argilic*
51		L' – M'	39	4	*Argilic*
52		M' – N'	39	4	*Argilic*
53		N' – O'	39	4	*Argilic*
54		O' – P'	39	4	*Argilic*
55		P' – Q'	39	4	*Argilic*
56		Q' – R'	39	4	*Argilic*
57		R' – S'	39	4	*Argilic*
58		S' – T'	39	4	*Argilic*
59		T' – U'	39	4	*Argilic*
60		U' – V'	39	4	*Argilic*
61		V' – W'	39	4	*Argilic*
62		W' – X'	54	3	*Argilic*
63		X' – Y'	54	3	*Argilic*
64		Y' – Z'	69	2	*Adv.Argilic*
65		Z' – AA'	54	3	*Argilic*
66		AA' – BB'	53	3	*Argilic*
67		BB' – CC'	67	2	*Adv.Argilic*
68		CC' – DD'	58	3	*Adv.Argilic*
69		DD' – EE'	33	4	*Argilic*
70		EE' – FF'	29	4	*Argilic*
71		FF' – GG'	38	4	*Argilic*
72	715	A' – B'	74	2	*Silicic*
73		B' – C'	74	2	*Silicic*
74		C' – D'	72	2	*Adv. Argilic*
75		D' – E'	72	2	*Adv. Argilic*
76		E' – F'	72	2	*Adv. Argilic*
77		F' – G'	52	3	*Adv. Argilic*
78		G' – H'	64	2	*Adv. Argilic*
79		H' – I'	64	2	*Adv. Argilic*
80		I' – J'	66	2	*Adv. Argilic*
81		J' – K'	64	2	*Adv. Argilic*
82		K' – L'	64	2	*Adv. Argilic*
83		L' – M'	64	2	*Adv. Argilic*
84		M' – N'	69	2	*Adv. Argilic*
85		N' – O'	54	3	*Argilic*
86		O' – P'	54	3	*Argilic*
87		P' – Q'	52	3	*Argilic*
88		Q' – R'	53	3	*Argilic*
89		R' – S'	50	3	*Argilic*
90		S' – T'	40	4	*Argilic*
91		T' – U'	40	4	*Argilic*
92		U' – V'	40	4	*Argilic*
93		V' – W'	40	4	*Argilic*
94		W' – X'	40	4	*Argilic*
95	705	A' – B'	77	2	*Silicic*
96		B' – C'	77	2	*Silicic*
97		C' – D'	71	2	*Adv. Argilic*
98		D' – E'	75	2	*Adv. Argilic*
99		E' – F'	58	3	*Silicic*

DOI : http://dx.doi.org/10.12962/j25023659.v11i1.1882

Artikel Masuk : 25-07-2024 Artikel Diulas : 13-11-2024 Artikel Diterima : 09-04-2025

100	F' – G'	50	3	*Silicic*
101	G' – H'	40	4	*Adv. Argilic*
102	H' – I'	28	4	*Silicic*
103	I' – J'	40	4	*Adv. Argilic*
104	J' – K'	40	4	*Adv. Argilic*
105	K' – L'	40	4	*Argilic*
106	L' – M'	40	4	*Argilic*
107	M' – N'	40	4	*Argilic*
108	N' – O'	40	4	*Argilic*
109	O' – P'	40	4	*Argilic*
110	P' – Q'	40	4	*Argilic*
111	Q' – R'	40	4	*Argilic*
112	R' – S'	40	4	*Argilic*
113	S' – T'	40	4	*Argilic*
114	T' – U'	40	4	*Argilic*
115	U' – V'	40	4	*Argilic*

Table 2. Estimated Monitoring Results of Deformation and Slope Movement Speed

No	Location	Segment	Alteration Type	Pixel Radar (X,Y)	Deformation Max (MM)	VCP 60 (MM/hour)	VCP 60 (MM/hour)	Risk
1	760	A' – B'	*Argilic*	-	-	-	-	*Lowrisk*
2		B' – C'	*Argilic*	-	-	-	-	*Lowrisk*
3		C' – D'	*Argilic*	118.69	6.3	3.4	2.5	*Mediumrisk*
4		D' – E'	*Adv. Argilic*	119.68	2.4	2.8	3.8	*Mediumrisk*
5		E' – F'	*Adv. Argilic*	-	-	-	-	*Lowrisk*
6		F' – G'	*Adv. Argilic*	-	-	-	-	*Lowrisk*
7		G' – H'	*Argilic*	-	-	-	-	*Lowrisk*
8		H' – I'	*Argilic*	-	-	-	-	*Lowrisk*
9		I' – J'	*Argilic*	-	-	-	-	*Lowrisk*
10	745	A' – B'	*Argilic*	-	-	-	-	*Lowrisk*
11		B' – C'	*Argilic*	-	-	-	-	*Lowrisk*
12		C' – D'	*Argilic*	-	-	-	-	*Lowrisk*
13		D' – E'	*Argilic*	126.65	7.3	2.9	3.9	*Mediumrisk*
14		E' – F'	*Argilic*	128.65	6.7	2.6	3	*Mediumrisk*
15		F' – G'	*Argilic*	-	-	-	-	*Lowrisk*
16		G' – H'	*Argilic*	-	-	-	-	*Lowrisk*
17		H' – I'	*Argilic*	-	-	-	-	*Lowrisk*
18		I' – J'	*Argilic*	-	-	-	-	*Lowrisk*
19		J' – K'	*Argilic*	-	-	-	-	*Lowrisk*
20		K' – L'	*Argilic*	-	-	-	-	*Lowrisk*
21		L' – M'	*Argilic*	-	-	-	-	*Lowrisk*
22		M' – N'	*Argilic*	-	-	-	-	*Lowrisk*
23		N' – O'	*Argilic*	-	-	-	-	*Lowrisk*
24		O' – P'	*Argilic*	-	-	-	-	*Lowrisk*
25		P' – Q'	*Argilic*	-	-	-	-	*Lowrisk*
26		Q' – R'	*Argilic*	-	-	-	-	*Lowrisk*
27		R' – S'	*Argilic*	-	-	-	-	*Lowrisk*
28		S' – T'	*Argilic*	-	-	-	-	*Lowrisk*

DOI : http://dx.doi.org/10.12962/j25023659.v11i1.1882

Artikel Masuk : 25-07-2024 Artikel Diulas : 13-11-2024 Artikel Diterima : 09-04-2025

29		T’ – U’	*Argilic*	-	-	-	-	*Lowrisk*
30		U’ – V’	*Argilic*	-	-	-	-	*Lowrisk*
31		V’ – W’	*Argilic*	-	-	-	-	*Lowrisk*
32		W’ – X’	*Argilic*	-	-	-	-	*Lowrisk*
33		X’ – Y’	*Argilic*	-	-	-	-	*Lowrisk*
34		Y’ – Z’	*Argilic*	-	-	-	-	*Lowrisk*
35		Z’ – AA’	*Argilic*	-	-	-	-	*Lowrisk*
36		AA’ – BB’	*Argilic*	-	-	-	-	*Lowrisk*
37		BB’ – CC’	*Argilic*	-	-	-	-	*Lowrisk*
38		CC’ – DD’	*Argilic*	-	-	-	-	*Lowrisk*
39		DD’ – EE’	*Argilic*	-	-	-	-	*Lowrisk*
40	730	A’ – B’	*Silicic*	-	-	-	-	*Lowrisk*
41		B’ – C’	*Silicic*	-	-	-	-	*Lowrisk*
42		C’ – D’	*Silicic*	-	-	-	-	*Lowrisk*
43		D’ – E’	*Adv. Argilic*	-	-	-	-	*Lowrisk*
44		E’ – F’	*Adv. Argilic*	-	-	-	-	*Lowrisk*
45		F’ – G’	*Adv. Argilic*	-	-	-	-	*Lowrisk*
46		G’ – H’	*Adv. Argilic*	-	-	-	-	*Lowrisk*
47		H’ – I’	*Adv. Argilic*	-	-	-	-	*Lowrisk*
48		I’ – J’	*Adv. Argilic*	-	-	-	-	*Lowrisk*
49		J’ – K’	*Adv. Argilic*	-	-	-	-	*Lowrisk*
50		K’ – L’	*Argilic*	-	-	-	-	*Lowrisk*
51		L’ – M’	*Argilic*	-	-	-	-	*Lowrisk*
52		M’ – N’	*Argilic*	-	-	-	-	*Lowrisk*
53		N’ – O’	*Argilic*	-	-	-	-	*Lowrisk*
54		O’ – P’	*Argilic*	-	-	-	-	*Lowrisk*
55		P’ – Q’	*Argilic*	-	-	-	-	*Lowrisk*
56		Q’ – R’	*Argilic*	-	-	-	-	*Lowrisk*
57		R’ – S’	*Argilic*	145.62	167	16	50	*Highrisk*
58		S’ – T’	*Argilic*	146.62	122	12	18	*Highrisk*
59		T’ – U’	*Argilic*	147.62	122.7	12	18.6	*Highrisk*
60		U’ – V’	*Argilic*	151.62	90	3	7.6	*Highrisk*
61		V’ – W’	*Argilic*	-	-	-	-	*Lowrisk*
62		W’ – X’	*Argilic*	-	-	-	-	*Lowrisk*
63		X’ – Y’	*Argilic*	152.62	260	4.4	25	*Highrisk*
64		Y’ – Z’	*Adv.Argilic*	153.6	335	3.4	3	*Mediumrisk*
65		Z’ – AA’	*Argilic*	155.61	121	4	17.9	*Mediumrisk*
66		AA’ –BB’	*Argilic*	-	-	-	-	*Lowrisk*
67		BB’ – CC’	*Adv.Argilic*	-	-	-	-	*Lowrisk*
68		CC’ – DD’	*Adv.Argilic*	-	-	-	-	*Lowrisk*
69		DD’ – EE’	*Argilic*	156.61	361	26	206	*Highrisk*
70		EE’ – FF’	*Argilic*	157.66	207	10.5	61.8	*Highrisk*
71		FF’ – GG’	*Argilic*	158.62	100.21	11.49	56	*Highrisk*
72	715	A’ – B’	*Silicic*	-	-	-	-	*Lowrisk*

DOI : http://dx.doi.org/10.12962/j25023659.v11i1.1882

Artikel Masuk : 25-07-2024 Artikel Diulas : 13-11-2024 Artikel Diterima : 09-04-2025

73		B' – C'	*Silicic*	-	-	-	-	*Lowrisk*
74		C' – D'	*Adv. Argilic*	-	-	-	-	*Lowrisk*
75		D' – E'	*Adv. Argilic*	-	-	-	-	*Lowrisk*
76		E' – F'	*Adv. Argilic*	-	-	-	-	*Lowrisk*
77		F' – G'	*Adv. Argilic*	-	-	-	-	*Lowrisk*
78		G' – H'	*Adv. Argilic*	-	-	-	-	*Lowrisk*
79		H' – I'	*Adv. Argilic*	-	-	-	-	*Lowrisk*
80		I' – J'	*Adv. Argilic*	-	-	-	-	*Lowrisk*
81		J' – K'	*Adv. Argilic*	-	-	-	-	*Lowrisk*
82		K' – L'	*Adv. Argilic*	-	-	-	-	*Lowrisk*
83		L' – M'	*Adv. Argilic*	-	-	-	-	*Lowrisk*
84		M' – N'	*Adv. Argilic*	-	-	-	-	*Lowrisk*
85		N' – O'	*Argilic*	-	-	-	-	*Lowrisk*
86		O' – P'	*Argilic*	-	-	-	-	*Lowrisk*
87		P' – Q'	*Argilic*	131.66	14.	2.9	2.4	*Mediumrisk*
88		Q' – R'	*Argilic*	132.66	5.6	3.3	2.6	*Mediumrisk*
89		R' – S'	*Argilic*	135.65	10.9	4.4	4.3	*Mediumrisk*
90		S' – T'	*Argilic*	136.65	6.9	3.9	3.6	*Mediumrisk*
91		T' – U'	*Argilic*	-	-	-	-	*Lowrisk*
92		U' – V'	*Argilic*	-	-	-	-	*Lowrisk*
93		V' – W'	*Argilic*	-	-	-	-	*Lowrisk*
94		W' – X'	*Argilic*	-	-	-	-	*Lowrisk*
95	705	A' – B'	*Silicic*	-	-	-	-	*Lowrisk*
96		B' – C'	*Silicic*	-	-	-	-	*Lowrisk*
97		C' – D'	*Adv. Argilic*	-	-	-	-	*Lowrisk*
98		D' – E'	*Adv. Argilic*	-	-	-	-	*Lowrisk*
99		E' – F'	*Silicic*	-	-	-	-	*Lowrisk*
100		F' – G'	*Silicic*	-	-	-	-	*Lowrisk*
101		G' – H'	*Adv. Argilic*	-	-	-	-	*Lowrisk*
102		H' – I'	*Silicic*	-	-	-	-	*Lowrisk*
103		I' – J'	*Adv. Argilic*	-	-	-	-	*Lowrisk*
104		J' – K'	*Adv. Argilic*	-	-	-	-	*Lowrisk*
105		K' – L'	*Argilic*	-	-	-	-	*Lowrisk*
106		L' – M'	*Argilic*	-	-	-	-	*Lowrisk*
107		M' – N'	*Argilic*	-	-	-	-	*Lowrisk*
108		N' – O'	*Argilic*	-	-	-	-	*Lowrisk*
109		O' – P'	*Argilic*	-	-	-	-	*Lowrisk*
110		P' – Q'	*Argilic*	124.62	9.7	3.5	3.9	*Mediumrisk*
111		Q' – R'	*Argilic*	126.62	6.6	3.1	3.6	*Mediumrisk*
112		R' – S'	*Argilic*	-	-	-	-	*Lowrisk*
113		S' – T'	*Argilic*	-	-	-	-	*Lowrisk*
114		T' – U'	*Argilic*	-	-	-	-	*Lowrisk*
115		U' – V'	*Argilic*	-	-	-	-	*Lowrisk*

DOI : http://dx.doi.org/10.12962/j25023659.v11i1.1882

Artikel Masuk : 25-07-2024 Artikel Diulas : 13-11-2024 Artikel Diterima : 09-04-2025

Meanwhile, observation photos and slope movement monitoring analysis results are presented in (Figure 1), and Slope Stability Radar pixel photos are presented in (Figure 2).

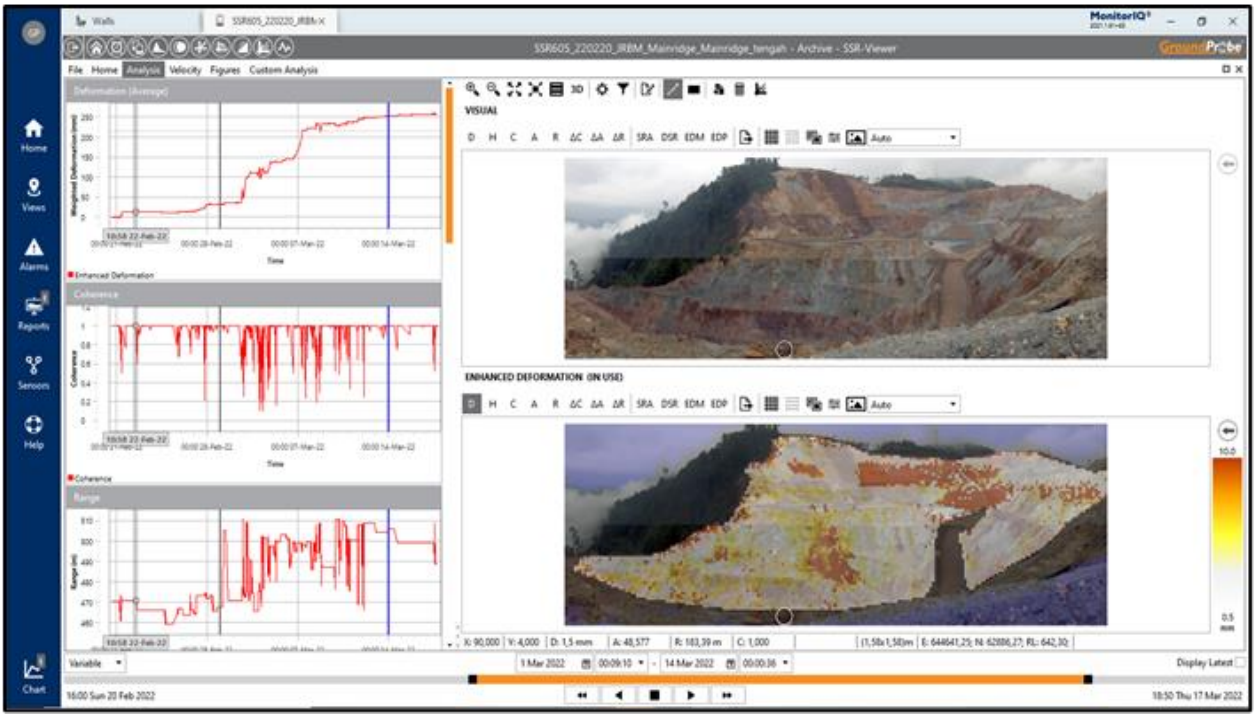

Figure 1. Observation photos and results of slope movement monitoring analysis (View MonitorIQ)

The default software from Groundprobe, MonitorIQ, reads the radar results algorithm. This software can visualize and facilitate real-time slope monitoring analysis and make back analyses of landslide events. There are several parameters of the main graphs for reading radar monitoring results, namely; Deformation: describes the movement of readings based on the wave phase difference compared to the previous reading. Amplitude: the strength of the radar signal reflected by the slope, based on the density of the reflecting surface. Range: The distance between the SSR and the slope based on the wave travel time. Coherence: comparison of the combination of several ranges and amplitudes that have changed in the previous scan. Velocity: the speed of movement of the mine slope towards or away from the radar. Inverse Velocity: an analysis technique used to predict landslide time whose value is the inverse of velocity.

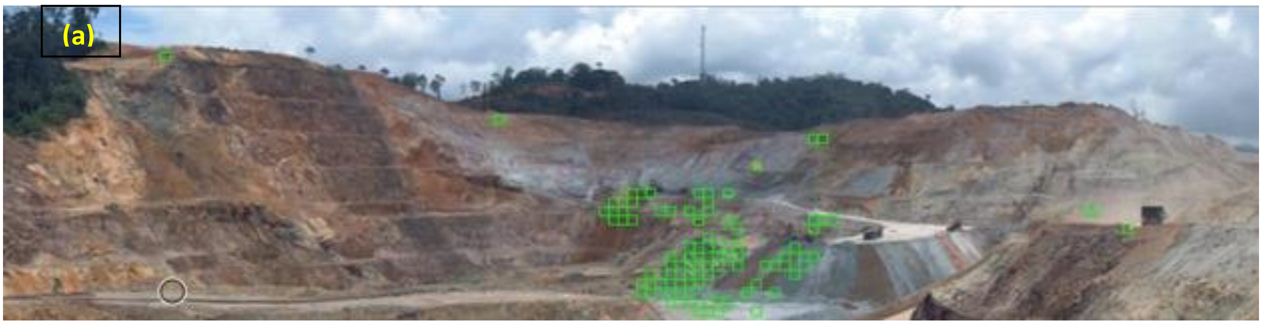

DOI : http://dx.doi.org/10.12962/j25023659.v11i1.1882

Artikel Masuk : 25-07-2024 Artikel Diulas : 13-11-2024 Artikel Diterima : 09-04-2025

Figure 2. Pixel photo (a) and Slope Stability Radar (SSR605-XT) (b)

Correlation Analysis of Radar Monitoring Results with RMR and Alteration Type Data

The research location on bench RL705-RL760 Pit Main Ridge North, as the location of the research object in this analysis, has various maximum deformations and velocities. Of the total 115 segments, seven segments are categorized as high risk (6%), 13 segments are categorized as medium risk (11.30%), and 95 segments are categorized as low risk (82.61%) (Figure 3).

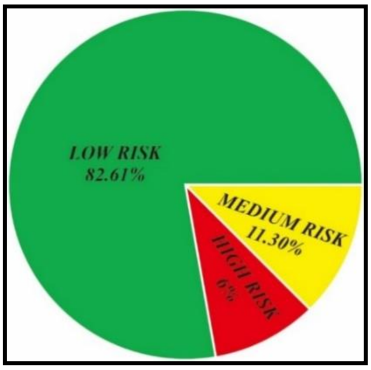

Figure 3. Landslide Risk Distribution Diagram

The classification results for each segment are correlated with the RMR zoning, so it can be seen that the high-risk category is in RMR class 4, while for RMR class 3 and Class 2, it is in moderate-low risk. An example of monitoring analysis in the 730DDEE segment was a linear-progressive-regressive deformation pattern on March 2- 6, 2022. The trend transition from linear-progressive is called the Onset of Failure time, precisely March 3, 2022, at 14.04 WITA with a maximum speed of 21mm/h (using VCP60) and 206mm/day (using VCP1440), is categorized as high-risk velocity. The deformation during the progressive phase is 361mm (Figure 4).

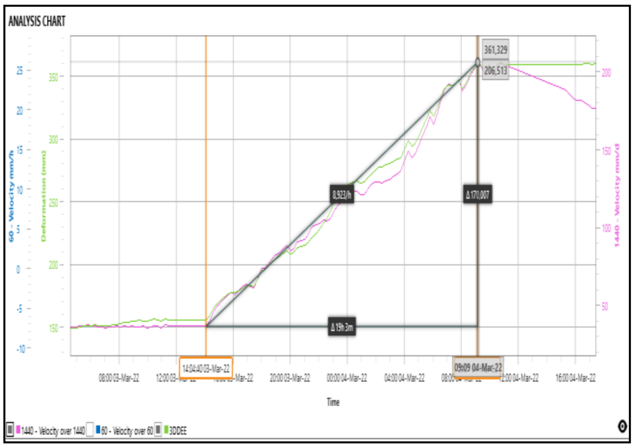

Figure 4. Deformation-Velocity-Time Graph on the 730DDEE Segment

DOI : http://dx.doi.org/10.12962/j25023659.v11i1.1882

Artikel Masuk : 25-07-2024 Artikel Diulas : 13-11-2024 Artikel Diterima : 09-04-2025

Landslides are geological disasters that often occur and cause significant losses globally. Evaluating slope stability somewhat is very important (Chen & Dai, 2021) so mitigation measures can be designed and implemented appropriately to avoid worsening slope damage (Al-E'Bayat et al., 2024). Based on the results of monitoring analysis and RMR estimation for each type of alteration in the research area, the landslide-prone zone is divided into 2: the safe zone and the landslide-prone zone. The safe zone includes the silicic and advanced argillic alteration zone, with an RMR value of more than 60 (Class 2) and a low-risk velocity value. Meanwhile, the argillic alteration zone includes the landslide-prone zone, with an RMR value of less than 60 (Class 3 and 4) and a high-risk velocity value. The criteria for each zone are shown in (Table 3).

Table 3. Criteria for Landslide Prone Areas

Criteria	Alteration Type	RMR	*Velocity*
Safe Zone	*Silicic, Advanced Argilic*	>60 Class 2	*Low* *Moderate*
Landslide Prone Zone	*Argilic*	< 60 Class 3,4	*High Risk*

Following is data from 115 segments analyzed (figure 5), there are 16 segments that are prone to landslides, namely:

a). 760 CD e). 730 ST i). 730 EEFF m). 715 RS

b). 760 DE f). 730 TU j). 730 FFGG n). 715 ST

c). 760 EF g). 730 XY k). 715PQ o). 705 PQ

d). 730 RS h). 730 DDEE l). 715QR p). 705 QR

The location map of 16 segments that are prone to landslides (high risk) in the red zone.

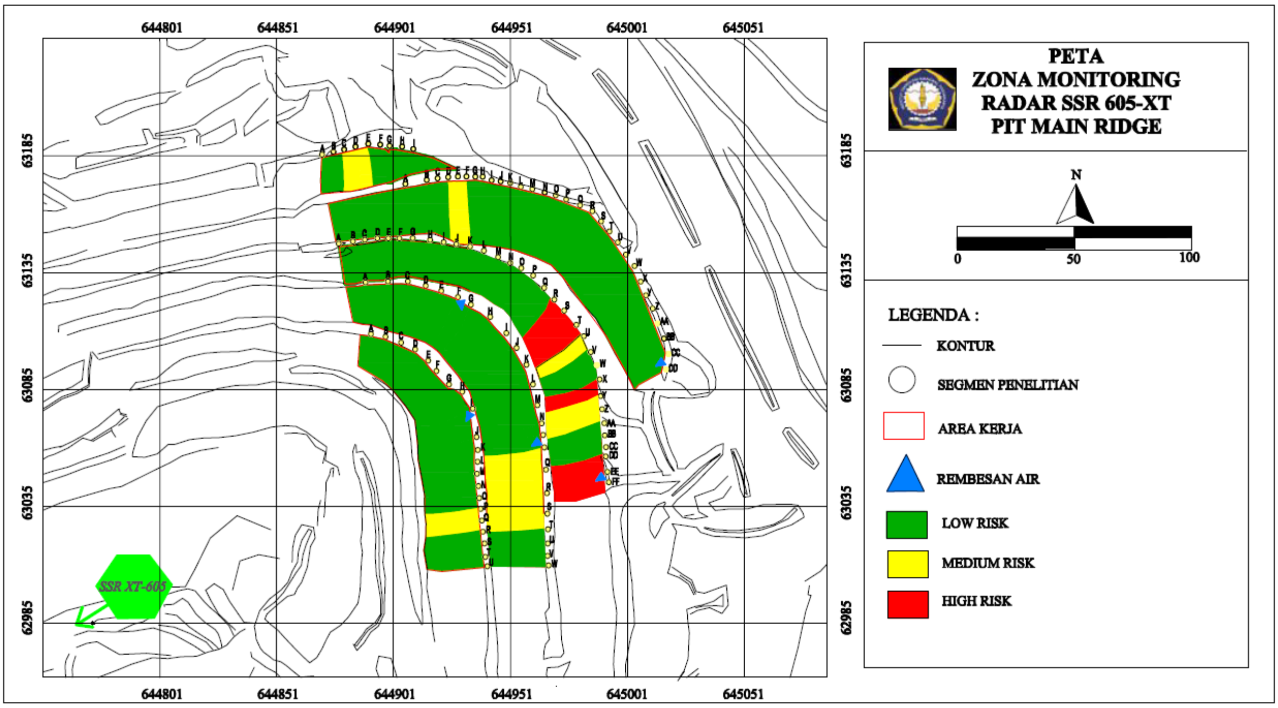

Figure 5. The Location Map of 115 Segments of Radar SSR 605-XT Monitoring, including 16 Segments that are Prone to Landslides (High Risk)

DOI : http://dx.doi.org/10.12962/j25023659.v11i1.1882

Artikel Masuk : 25-07-2024 Artikel Diulas : 13-11-2024 Artikel Diterima : 09-04-2025

CONCLUSION

The findings from monitoring slope movement using slope stability radar indicate that the stability level of the mine slope is influenced by the characteristics of the rock mass and the type of alteration. In the study area, the safety zone for potential landslides in the North Main Ridge Pit corresponds to RMR class 2, characterized by an RMR rating value exceeding 60, and exhibits low-risk velocities in advanced argillic and silicic alteration types. Conversely, the landslide-prone zone in the North Main Ridge Pit falls within RMR classes 3–4, with an RMR value below 60, and demonstrates high-risk velocities in the argillic alteration type. Future investigations could leverage technologies like artificial intelligence (AI) to assess slope stability, as AI has demonstrated its ability to forecast safety factors for land slopes under both static and seismic loads (Khajehzadeh et al., 2022).

ACKNOWLEDGMENTS

The authors are grateful to PT. J Resources Bolaang Mongondow for providing the data of the research

REFERENCES

Abd Rahim, I., Musta, B., & Abdullah, R. F. (2023). Application of Modified Slope Mass Rating (M-SMR) System in Ultrabasic Rock: A Case Study in Telupid, Sabah, Malaysia. Indonesian Journal on Geoscience, 10(1), 63-71.

Adhitama, W., Wijaya, R. A. E., & Putra, B. 2021, October. Muckpiles Influence Againts Pillar Stability in Panel 26 and 27 West Drawpoint 43-44 Grasberg Block Cave (GBC) PT. Freeport Indonesia. In Proceedings of the 2nd International Conference on Industrial and Tzechnology and Information Design, ICITID 2021, 30 August 2021, Yogyakarta, Indonesia.

Al-E'Bayat, M., Guner, D., Sherizadeh, T., & Asadizadeh, M. (2024). Numerical Investigation for the Effect of Joint Persistence on Rock Slope Stability Using a Lattice Spring-Based Synthetic Rock Mass Model. Sustainability, 16(2), 894.

Azarafza, M., Akgün, H., Ghazifard, A., Asghari-Kaljahi, E., Rahnamarad, J., & Derakhshani, R. (2021). Discontinuous rock slope stability analysis by limit equilibrium approaches–a review. International Journal of Digital Earth, 14(12), 1918-1941.

Bieniawski, Z. T. (1989). Engineering rock mass classifications: a complete manual for engineers and geologists in mining, civil, and petroleum engineering. John Wiley & Sons.

Boyle, A., Wilkinson, P., Chambers, J., Lesparre, N., & Adler, A. 2014. 15th International Conference on Biomedical Applications of Electrical Impedance Tomography, Gananoque, Canada.

Chen, X., Jiang, H., Chen, L., Du, W., & Gong, S. (2023). Experimental Study on Creep Characteristics of Unloaded Rock Masses for Excavation of Rock Slopes in Cold Areas. Applied Sciences, 13(5), 3138.

Chen, Z. Y., & Dai, Z. H. (2021). Application of group decision-making AHP of confidence index and cloud model for rock slope stability evaluation. Computers & Geosciences, 155, 104836.

Delgado-Reivan, X., Paredes-Miranda, C., Loaiza, S., Echeverria, M. D. P. V., Mulas, M., & Jordá-Bordehore, L. (2023). Stability Analysis of Rocky Slopes on the Cuenca–Girón–Pasaje Road, Combining Limit Equilibrium Methods, Kinematics, Empirical Methods, and Photogrammetry. Remote Sensing, 15(3), 862.

Elmouttie, M., & Dean, P. (2020). Systems engineering approach to slope stability monitoring in the digital mine. Resources, 9(4), 42.

Ganesan, G., & Mishra, A. K. (2024). Development of a directional continuous joint adjustment rating for the rock mass rating system. Arabian Journal of Geosciences, 17(2), 1-13.

Gong, W., Bowa, V. M., Zhao, C., Cheng, Z., & Zhang, L. (2021). Footwall Rock Slope Stability Evaluations at Nchanga Open Pit Mine, Zambia. Geotechnical and Geological Engineering, 39(8), 5753-5765.

Huang, Y., Zhang, J., Li, B., & Chen, S. (2024). Slope Stability Analysis and Soil Mechanical Properties of Impact Craters around the Lunar South Pole. Remote Sensing, 16(2), 371.

DOI : http://dx.doi.org/10.12962/j25023659.v11i1.1882

Artikel Masuk : 25-07-2024 Artikel Diulas : 13-11-2024 Artikel Diterima : 09-04-2025

Indriastuty, D., Fajar, F., Tappang, G., & Irsyad, A. (2021). Pemantauan Deformasi Lereng Tambang Terbuka Paska Peledakan dengan Slope Stability Radar. Indonesian Mining Professionals Journal, 3(2), 71-82.

Jaiswal, A., Verma, A. K., & Singh, T. N. (2024). Evaluation of slope stability through rock mass classification and kinematic analysis of some major slopes along NH-1A from Ramban to Banihal, North Western Himalayas. Journal of Rock Mechanics and Geotechnical Engineering, 16(1), 167-182.

Jia, L., Cai, J., Wu, L., Qin, T., & Song, K. (2023). Influence of Fracture Geometric Characteristics on Fractured Rock Slope Stability. Applied Sciences, 13(1), 236.

Khajehzadeh, M., Taha, M. R., Keawsawasvong, S., Mirzaei, H., & Jebeli, M. (2022). An effective artificial intelligence approach for slope stability evaluation. Ieee Access, 10, 5660-5671.

Kumar, A. (2020). Time-domain reflectometry–based real-time slope stability monitoring in opencast mines: A review. Noise & Vibration Worldwide, 0957456520924812.

Kumar A. & Rathee, R. (2017). Monitoring and evaluating of slope stability for setting out of critical limit at slope stability radar, International Geo-Engineering.

Kumar, S., Choudhary, S. S., & Burman, A. (2023). Recent advances in 3D slope stability analysis: a detailed review. Modeling Earth Systems and Environment, 9(2), 1445-1462.

Kundu, J., Sarkar, K., Ghaderpour, E., Scarascia Mugnozza, G., & Mazzanti, P. (2023). A GIS-Based Kinematic Analysis for Jointed Rock Slope Stability: An Application to Himalayan Slopes. Land, 12(2), 402.

Liu, Z., Liu, P., Zhou, C., & Zhang, L. (2021). A theoretical framework for optimization of three-dimensional slope stability monitoring. Engineering Geology, 295, 106436.

Martinelli, G., Pierotti, L., Facca, G., & Gherardi, F. (2023). Geofluids as a possible unconventional tool for seismic hazard assessment. Frontiers in Earth Science, 11, 1286817.

Moayedi, H., Osouli, A., Nguyen, H., & Rashid, A. S. A. (2021). A novel Harris hawks' optimization and k-fold cross-validation predicting slope stability. Engineering with Computers, 37, 369-379.

Oliveira, D. A., & Lana, M. S. (2023). Three-dimensional stability analyses and sensitivity studies of the input parameters in a global failure of an open pit slope: a case study. Arabian Journal of Geosciences, 16(3), 151.

PT. J Resources Bolaang Mongondow. 2022, Pit Main Ridge Utara Geotechnical Domain Database. Departemen Geoteknik, PT. J Resources Bolaang Mongondow

Qazi, A., & Singh, K. (2023). Rock Mass Classification Techniques and Parameters: A Review. Journal of Mining and Environment.

Reeves, B., Noon, D. A., Stickley, G. F., & Longstaff, D. (2001, November). Slope stability radar for monitoring mine walls. In Subsurface and Surface Sensing Technologies and Applications III (Vol. 4491, pp. 57-67). SPIE.

Saunders, P., Nicoll, S., & Christensen, C. (2016, September). Slope stability radar alarm threshold validation at Telfer gold mine. In APSSIM 2016: Proceedings of the First Asia Pacific Slope Stability in Mining Conference (pp. 367-378). Australian Centre for Geomechanics.

Saunders, P., Kabuya, J., Torres, A., & Simon, R. (2020, May). Post-blast slope stability monitoring with slope stability radar. In International Symposium on Slope Stability in Open Pit Mining and Civil Engineering, Perth.

Shellam, R., & Coggan, J. (2020, May). Analysis of velocity and acceleration trends using slope stability radar to identify failure 'signatures' to better inform deformation trigger action response plans. In Slope Stability 2020: Proceedings of the 2020 International Symposium on Slope Stability in Open Pit Mining and Civil Engineering (pp. 227-240). Australian Centre for Geomechanics.

Singh, K., & Kumar, V. (2020). Road-cut Slope Stability Assessment along Himalayan National Highway NH-154A, India. Journal of the Geological Society of India, 96, 491-498.

Singh, P., Bardhan, A., Han, F., Samui, P., & Zhang, W. (2023). A critical review of conventional and soft computing methods for slope stability analysis. Modeling Earth Systems and Environment, 9(1), 1-17.

Sulistio, D. S. D., & Wijaya, A. E. (2022). Analisis Monitoring Pergerakan Lereng Timbunan Quarry Batugamping di PT. Cicatih Putra Sukabumi. Mining Insight, 3(1), 21-32.

DOI : http://dx.doi.org/10.12962/j25023659.v11i1.1882

Artikel Masuk : 25-07-2024 Artikel Diulas : 13-11-2024 Artikel Diterima : 09-04-2025

Vasilev and Toshkov, 2016, Slope Stability Monitoring at Ellatzite Open pit, Технологии и практики при подземен добив и минно строителство, 4 – 7 октомври 2016, Девин, България.

Wardana, N., & Wijaya, R. A. E. (2021, October). Analysis Of Block Stability For Room And Pillar Coal Mining In Pillar Panel Using Numerical Methods. In Proceedings of the 2nd International Conference on Industrial and Technology and Information Design, ICITID 2021, 30 August 2021, Yogyakarta, Indonesia.

Wang, T., Zhang, W., Li, J., Liu, D., & Zhang, L. (2024). Identification of Complex Slope Subsurface Strata Using Ground-Penetrating Radar. Remote Sensing, 16(2), 415.

Wijaya, R. A. E., & Isnawan, D. (2015). Analisis Kekuatan Massa Batugamping Dengan Menggunakan Kaidah Hoek-Brown Failure Criterion-Roclab di Daerah Gunung Sudo Kabupaten Gunung Kidul Yogyakarta. Promine, 3(1).

Wijaya, R. A. E., Karnawati, D., Srijono, S., & Wilopo, W. (2014). ROCK MASS RATING OF CAVITY LIMESTONE LAYER IN REMBANG, CENTRAL JAVA, INDONESIA. Journal of Applied Geology, 6(1).

Wu, A., Zhao, W., Zhang, Y., & Fu, X. (2023a). A detailed study of the CHN-BQ rock mass classification method and its correlations with RMR and Q system and Hoek-Brown criterion. International Journal of Rock Mechanics and Mining Sciences, 162, 105290.

Wu, F., Wu, J., Bao, H., Bai, Z., Qiao, L., Zhang, F., ... & Liu, C. (2023b). Rapid intelligent evaluation method and technology for determining engineering rock mass quality. Rock Mechanics Bulletin, 2(2), 100038.

Yang, Z., Ding, X., Liu, X., Wahab, A., Ao, Z., Tian, Y., ... & Ma, P. (2024). Slope Deformation Mechanisms and Stability Assessment under Varied Conditions in an Iron Mine Waste Dump. Water, 16(6), 846.

Zheng, B., Wang, J., Feng, S., Yang, H., Wang, W., Feng, T., & Hu, T. (2024). A new, fast, and accurate algorithm for predicting soil slope stability based on sparrow search algorithm-back propagation. Natural Hazards, 120(1), 297-319.

DOI : http://dx.doi.org/10.12962/j25023659.v11i1.1882

Artikel Masuk : 25-07-2024 Artikel Diulas : 13-11-2024 Artikel Diterima : 09-04-2025